

# Tetrahydrofolic Acid Is a Potent Suicide Substrate of Mushroom Tyrosinase

Francisco García-Molina,<sup>†</sup> Jose Luis Muñoz-Muñoz,<sup>†</sup> Francisco Martínez-Ortiz,<sup>‡</sup> Pedro Antonio García-Ruiz,<sup>§</sup> Jose Tudela,<sup>†</sup> Francisco García-Cánovas,<sup>\*,†</sup> and Jose Neptuno Rodríguez-López<sup>†</sup>

<sup>†</sup>Grupo de Investigación de Enzimología (GENZ), Departamento de Bioquímica y Biología Molecular-A, Facultad de Biología, Universidad de Murcia, Espinardo, Murcia E-30100, Spain

<sup>‡</sup>Grupo de Investigación de Electroquímica Teórica y Aplicada, Departamento de Física-Química, Facultad de Química, Universidad de Murcia, Espinardo, Murcia E-30100, Spain

<sup>§</sup>Grupo de Química de Carbohidratos y Tecnología de Alimentos (QCBA), Departamento de Química Orgánica, Facultad de Química, Universidad de Murcia, Espinardo, Murcia E-30100, Spain

**S** Supporting Information

**ABSTRACT:** The coenzyme tetrahydrofolic acid is the most rapid suicide substrate of tyrosinase that has been characterized to date. A kinetic study of the suicide inactivation process provides the kinetic constants that characterize it:  $\lambda_{\max}$ , the maximum apparent inactivation constant;  $r$ , the partition ratio or the number of turnovers made by one enzyme molecule before inactivation; and  $k_{\text{cat}}$  and  $K_m$ , the catalytic and Michaelis constants, respectively. From these values, it is possible to establish the ratio  $\lambda_{\max}/K_m$ , which represents the potency of the inactivation process. Besides acting as a suicide substrate of tyrosinase, tetrahydrofolic acid reduces *o*-quinones generated by the enzyme in its action on substrates, such as L-tyrosine and L-DOPA (*o*-dopaquinone), thus inhibiting enzymatic browning.

**KEYWORDS:** Tetrahydrofolic acid, tyrosinase, mechanism, suicide, inactivation

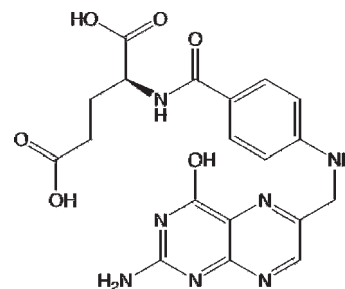
## INTRODUCTION

Tyrosinase (TYR) or polyphenol oxidase (monophenol, *o*-diphenol; oxygen-oxidoreductase; EC 1.14.18.1), which has two copper atoms in its active site, is ubiquitously present in biological systems. It catalyzes the oxidation of *o*-diphenols (diphenolase or catecholase activity) to the corresponding *o*-quinones through the consumption of molecular oxygen. It may also catalyze the regioselective *ortho*-hydroxylation of monophenols to catechols (monophenolase or cresolase activity) and their subsequent oxidation to *o*-quinones.<sup>1,2</sup> In animals, TYR triggers the biosynthesis of melanins in skin, hair, and eyes.<sup>1</sup> In plants,<sup>3</sup> fungi,<sup>4</sup> and bacteria,<sup>5</sup> this enzyme is involved in enzymatic browning,<sup>3</sup> a phenomenon that also acts as a defense against predators because of the toxicity of the intermediates of melanogenesis, such as *o*-quinones. TYR inhibitors are used as depigmenting agents.<sup>6–8</sup>

Folic acid or pteroil-L-glutamic acid is also known as B9 or M vitamin. *In vivo*, folic acid is reduced to dihydrofolic acid and, subsequently, to 5,6,7,8-tetrahydrofolic acid (THF; Scheme 1).<sup>9</sup> Folates are a class of compounds with a similar chemical structure and nutritional activity to folic acid and are found in vegetables, such as spinach, lettuce, etc., and fungi, such as mushrooms.<sup>10</sup>

The synthesis of many compounds and the regulation of metabolic processes require the addition or elimination of 1-carbon units ( $C_1$  metabolism).<sup>11</sup> These one-carbon reactions play essential roles in major cellular processes, including the synthesis of nucleic acids, methionine, and pantothenate, and other products, such as choline, lignine, and chlorophyll.<sup>11</sup> THF derivatives and S-adenosylmethionine mediate most of these transfers of  $C_1$

Scheme 1. Chemical Structure of THF



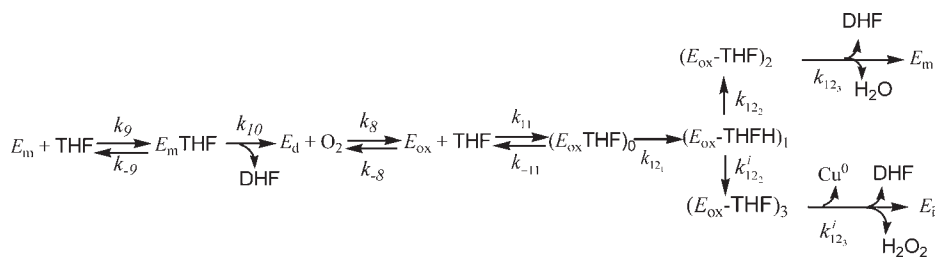
units. Only the tetra-reduced form of the folic acid serves as a coenzyme for  $C_1$ -transfer reactions.<sup>12</sup> Some of the initial steps of THF synthesis are absent in animals, and the folates required by these organisms are contributed by the diet.<sup>13,14</sup> Folate deficiency may have severe repercussions for human health (e.g., neural tube defects, heart coronary disease, or an increased risk of cancer). In contrast, microorganisms and plants are able to synthesize THF *de novo*.<sup>12</sup> Some drugs interfere with folic acid biosynthesis and, consequently, with THF, among them many inhibitors

**Received:** September 13, 2010

**Accepted:** December 22, 2010

**Revised:** December 21, 2010

**Published:** January 25, 2011

Scheme 2. Kinetic Mechanism To Explain the Suicide Inactivation of TYR in Its Action on THF, Where E<sub>i</sub> Is the Inactive Enzyme

of dihydrofolate reductase that have been used as antineoplastic agents, such as metotrexate and trimetoxate.<sup>15</sup> On the other hand, THF and its derivatives have been characterized as showing high antioxidant activity.<sup>9</sup> Moreover, this antioxidant activity is pH-dependent, as recently demonstrated.<sup>10</sup>

THF can affect the diphenolase and monophenolase activities of TYR,<sup>16</sup> as occurs with reduced nicotinamide adenine dinucleotide (NADH)<sup>17</sup> and 5,6,7,8-tetrahydrobiopterin<sup>18</sup> when it acts as a reductant of *o*-dopaquinone produced from 4-hydroxyphenylalanine (L-tyrosine) or 3,4-dihydroxyphenylalanine (L-DOPA) by TYR. As in the case of NADH<sup>17</sup> or 5,6,7,8-tetrahydrobiopterin,<sup>18</sup> THF can shorten the lag period of the monophenolase activity of TYR.<sup>16</sup> Moreover, in humans, serum levels of THF are related to the level of homocysteine; for example, at low levels of THF, the concentration of homocysteine increases to such an extent that it could inhibit TYR, a process that is related to psoriasis and vitiligo.<sup>19–21</sup>

Recently, the study of TYR inhibitors<sup>8</sup> and suicide substrates<sup>22,23</sup> has intensified the desire to take advantage of its depigmentation properties. Among the most powerful suicide substrates described in the literature, there are two isoflavone metabolites, 7,8,4'-trihydroxyisoflavone and 5,7,8,4'-tetrahydroxyisoflavone,<sup>22</sup> although 8-hydroxynaringenin, a biotransformed metabolite of naringenin,<sup>23</sup> has also been described as a suicide substrate. On the basis of such studies, it is proposed that 7,8,4'-trihydroxyl groups on flavonoid skeletons play important roles in producing the suicide inactivation of mushroom TYR. In this work, we make a kinetic study of THF as a suicide substrate of TYR and, at the same time, consider its effect on enzyme browning.

## MATERIALS AND METHODS

**Enzyme Source.** Mushroom TYR (3300 units/mg) from Sigma (Madrid, Spain) was purified as described in ref 24.

**Reagents.** L-Tyrosine, L-DOPA, and 4-*tert*-butylcatechol (TBC) were obtained from Aldrich (Madrid, Spain). 5,6,7,8-Tetrahydrofolic acid (THF) and 7,8-dihydrofolic acid (DHF) was purchased from Sigma (Madrid, Spain). Stock solutions of the diphenolic compounds and THF and DHF were prepared in phosphoric acid (0.15 mM). Protein concentrations were determined using Bradford's method,<sup>25</sup> using bovine serum albumin as the standard. Milli-Q System water was used throughout this work (Millipore, Billerica, MA).

**Monophenolase Activity of TYR.** The monophenolase activity of TYR was followed spectrophotometrically, measuring the accumulation of dopachrome at a wavelength of 475 nm ( $\epsilon = 3600 \text{ M}^{-1} \text{ cm}^{-1}$ )<sup>26</sup> during the oxidation of L-tyrosine, using a Perkin-Elmer  $\lambda$ -35 spectrophotometer connected to a personal computer (PC) (Perkin-Elmer, Waltham, MA). The conditions of the assay are specified in the corresponding figure captions.

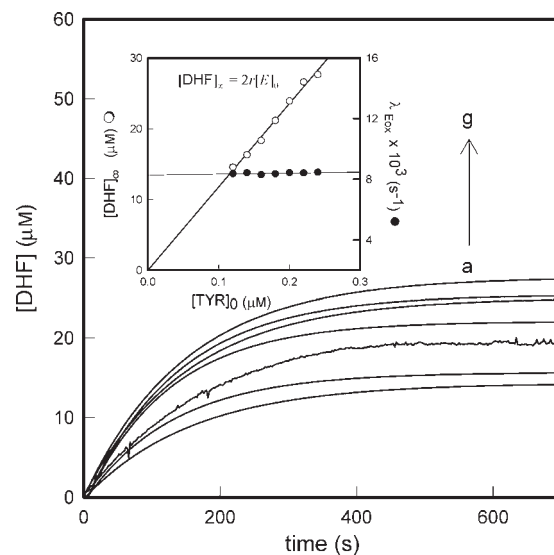


**Figure 1.** Representation of the variation in the concentration of DHF with respect to time during the suicide inactivation of TYR in its action on THF. The data were obtained for various enzyme concentrations. The conditions were 30 mM sodium phosphate buffer (pH 7.0),  $[\text{THF}]_0 = 0.31 \text{ mM}$ , and  $[\text{O}_2]_0 = 0.26 \text{ mM}$ , while enzyme concentrations (nM) were (a) 120, (b) 140, (c) 160, (d) 180, (e) 200, (f) 220, and (g) 240. (Inset) Corresponding values of (○)  $[\text{DHF}]_\infty$  and (●)  $\lambda_{E_{\text{ox}}}^{\text{THF}}$  for various concentrations of TYR.

**Diphenolase Activity of TYR.** The diphenolase activity of TYR was followed spectrophotometrically, measuring the accumulation of 4-*tert*-butyl-*o*-benzoquinone at a wavelength of 410 nm ( $\epsilon = 1200 \text{ M}^{-1} \text{ cm}^{-1}$ )<sup>26</sup> during the oxidation of TBC or measuring the accumulation of dopachrome at a wavelength of 475 nm ( $\epsilon = 3600 \text{ M}^{-1} \text{ cm}^{-1}$ )<sup>26</sup> during the oxidation of L-DOPA, using the above-mentioned apparatus. The assay conditions are specified in the corresponding figure captions.

**THF Oxidase Activity. Oximetric Measurements.** The values of  $V_{0,\text{THF}}^{\text{O}_2}$  were determined at short reaction times in triplicate at each  $[\text{THF}]_0$ .<sup>27</sup> From experiments in which the dependence of  $V_{0,\text{THF}}^{\text{O}_2}$  upon  $[\text{THF}]_0$  was studied,  $V_{\text{max}}^{\text{O}_2}$  and  $K_m^{\text{THF}}$  were obtained by nonlinear regression fitting of the data for  $V_{0,\text{THF}}^{\text{O}_2}$  versus  $[\text{THF}]_0$ , using the Sigma Plot program for Windows.<sup>28</sup>

**Spectrophotometric Measurements.** The initial  $V_{0,\text{THF}}^{\text{DHF}}$  rates were obtained by measuring the increase in absorbance at 340 nm. The  $\Delta\epsilon_{340}$  values of THF after conversion into DHF were calculated at the different pH values used, using equal concentrations of THF and DHF and measuring the absorbance at each pH (pH 9.2, 8.5, 8.0, 7.5, 7.0, 6.5, 6.0, 5.5, 5.0, 4.5, 4.0, 3.5, 3.2, 3.0, 2.75, 2.5, and 2.2), giving 4270, 4210, 4020, 4005, 3890, 3710, 3440, 2810, 2000, 1950, 1865, 1850, 1810, 1808, 1807, 1804, and  $1801 \text{ M}^{-1} \text{ cm}^{-1}$ , respectively. When the pH was varied, 30 mM

**Table 1. Kinetic Constants That Characterize the Suicide Inactivation of TYR by THF and Values of the Chemical Shifts of THF Obtained by  $^{13}\text{C}$  NMR for the Carbons  $\text{C}_4$  and  $\text{C}_{4a}$  at pH 7.0**

substrate	$\lambda_{E_{ox}(\max)} (\times 10^3, \text{s}^{-1})$	$r = k_{\text{cat}}/\lambda_{E_{ox}(\max)}$	$k_{\text{cat}} (\text{s}^{-1})$	$K_m^{\text{THF}} (\text{mM})$	$K_m^{\text{O}_2} (\mu\text{M})$	$\lambda_{E_{ox}(\max)}/K_m^{\text{THF}} (\text{mM}^{-1} \text{s}^{-1})$	$\delta_{4a} (\text{ppm})$	$\delta_4 (\text{ppm})$
THF	$30 \pm 2$	$59.7 \pm 4.3$	$1.79 \pm 0.21$	$0.62 \pm 0.07$	$0.031 \pm 0.005$	$0.048 \pm 0.07$	81.0	169.78

sodium acetate buffer was used for values between pH 2.2 and 5.0 and 30 mM sodium phosphate buffer was used for values between pH 5.5 and 9.2.

**Kinetics of the Suicide Inactivation.** The kinetics of the suicide inactivation of TYR in its action on THF can be followed by measuring oxygen consumption in an oxygraph or measuring the formation of DHF in a spectrophotometer. These spectrophotometric assays were carried out as described previously. The experimental data for the formation of DHF with time follow the equation

$$[\text{DHF}] = [\text{DHF}]_{\infty} (1 - e^{-\lambda_{E_{ox}}^{\text{THF}} t}) \quad (1)$$

where  $[\text{DHF}]$  is the instantaneous concentration of DHF,  $[\text{DHF}]_{\infty}$  is the DHF formed at the end of the reaction,  $t \rightarrow \infty$ , and  $\lambda_{E_{ox}}^{\text{THF}}$  is the apparent inactivation constant for  $E_{ox}$  in the suicide inactivation of TYR under aerobic conditions (Scheme 2).

**Square Wave Voltammograms (SWVs).** SWVs were recorded with a computer-driven three electrode potentiostat constructed in the "Research Support Service of the University of Murcia" (<http://www.um.es/sai>). The reference electrode was a saturated calomel electrode (SCE), and the counter electrode was a platinum wire. The oxidation was carried out on a home made graphite disk electrode (0.5 mm diameter), which was used in all of the experiments presented herein.

During square wave voltammetry, the net current was always recorded and a triangular scan was applied from an initial potential to a more positive potential, followed by a return to the initial potential. This triangular scan was preferred to the usual linear scan because the formal potential of a reversible process coincides with the peak potential in both direct and reverse scans, while for a quasi-reversible process, the formal potential lies between both peaks, allowing for accurate determination of this parameter.<sup>29</sup> The experimental conditions were 0.5 mM THF in 30 mM sodium acetate buffer (pH 4.5) or 30 mM sodium phosphate buffer (pH 7.0) at 25 °C, with square-wave potential,  $E_{\text{SW}}$ , 50 mV; potential increment,  $\Delta E$ , 1 mV; and square-wave period,  $\tau_{\text{SW}}$ , 50 ms.

**$^{13}\text{C}$  Nuclear Magnetic Resonance (NMR) Assays.** The  $^{13}\text{C}$  NMR spectrum of THF was obtained in a Varian Unity spectrometer at 600 MHz, using 30 mM sodium phosphate as buffer (pH 7.0) and  $^2\text{H}_2\text{O}$  as solvent. Chemical displacement ( $\delta$ ) values were measured relative to those for tetramethylsilane ( $\delta = 0$ ). The maximum line width accepted in the  $^{13}\text{C}$  NMR spectra was 0.06 Hz. Therefore, the maximum accepted error for each peak of the spectrum was  $\pm 0.03$  ppm.

## RESULTS AND DISCUSSION

**Suicide Inactivation of TYR in Its Action on THF.** THF can be oxidized by TYR, a process during which the enzyme undergoes suicide inactivation. The kinetic mechanism proposed to explain this suicide inactivation of TYR acting on THF is described in Scheme 2 and is based on the mechanism proposed to explain the action of the enzyme on *o*-diphenols.<sup>30</sup> Derivation of the analytical expression establishing the variation of the product (DHF) concentration with time when  $[\text{THF}]_0 \gg [\text{E}]_0$  is described in detail in the Supporting Information of ref 30.

On the basis of the findings of previous studies of the suicide inactivation of TYR from diverse sources, the process follows first-order kinetics and has a much higher partition ratio ( $r$ ) than 1.<sup>30</sup>

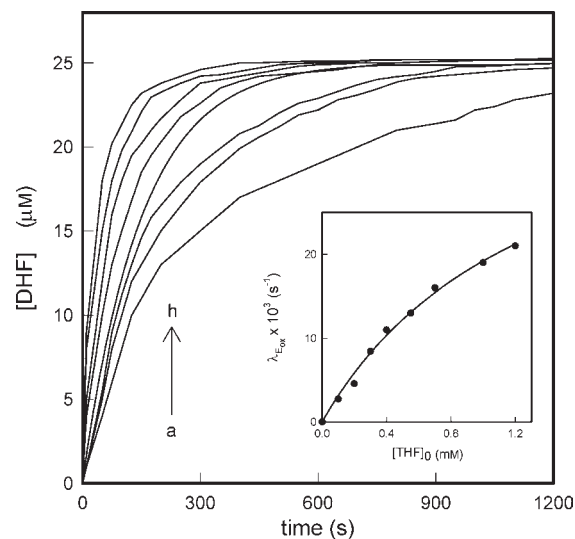


**Figure 2.** Representation of the variation in the concentration of DHF with respect to time during the suicide inactivation of TYR in its action on THF. The data were obtained for various substrate concentrations. The conditions were 30 mM sodium phosphate buffer (pH 7.0),  $[\text{O}_2]_0 = 0.26$  mM, and  $[\text{TYR}]_0 = 220$  nM, while substrate concentrations (mM) were (a) 0.1, (b) 0.2, (c) 0.3, (d) 0.4, (e) 0.55, (f) 0.7, (g) 1, and (h) 1.2. (Inset) Corresponding values of ( $\bullet$ )  $\lambda_{E_{ox}}^{\text{THF}}$  for various concentrations of THF.

The variation of  $[\text{DHF}]$  with time is given by eq 1, and therefore, when  $t \rightarrow \infty$ ,  $[\text{DHF}]$  has the following expression:

$$[\text{DHF}]_{\infty} = \frac{2k_{\text{cat}}}{\lambda_{E_{ox}(\max)}^{\text{THF}}} [\text{E}]_0 = \frac{2k_{12}}{k_{12}^i} [\text{E}]_0 = 2r[\text{E}]_0 \quad (2)$$

where  $k_{\text{cat}}$  and  $\lambda_{E_{ox}(\max)}^{\text{THF}}$  are the catalytic constant and the maximum inactivation constant, respectively, and  $r$  is the partition ratio between the catalytic pathway and the inactivation pathway and also called the number of turnovers realized by 1 mol of enzyme before its inactivation (Scheme 2). Keeping in mind that  $K_m^{\text{O}_2}$  values are very low<sup>31</sup> and that the initial concentration of  $\text{O}_2$  is 0.26 mM, the enzyme is saturated by  $\text{O}_2$ , and therefore, the following equation can be deduced for the variation of the apparent inactivation constant,  $\lambda_{E_{ox}}^{\text{THF}}$ , with the concentration of THF:

$$\lambda_{E_{ox}}^{\text{THF}} = \frac{\lambda_{E_{ox}(\max)}^{\text{THF}} [\text{THF}]_0}{K_m^{\text{THF}} + [\text{THF}]_0} \quad (3)$$

The variation in the initial velocity of DHF formation with respect to the concentration of THF is

$$V_{0,\text{THF}}^{\text{DHF}} = \frac{2k_{\text{cat}} [\text{THF}]_0 [\text{E}]_0}{K_m^{\text{THF}} + [\text{THF}]_0} \quad (4)$$

where  $K_m^{\text{THF}}$  is the Michaelis constant of TYR for THF.

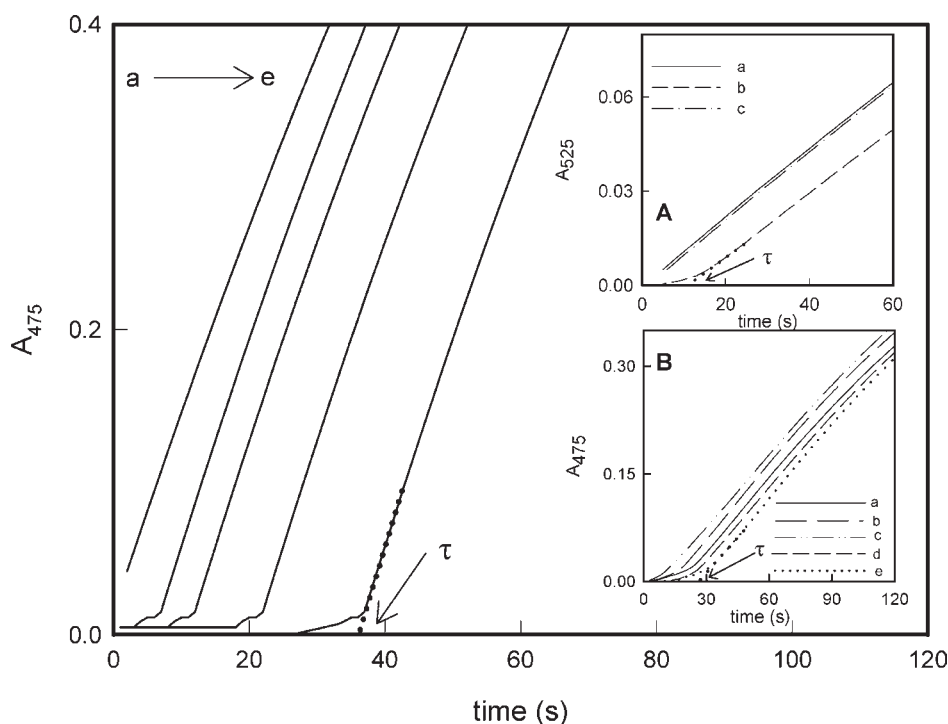


**Figure 3.** Action of THF on diphenolase activity of TYR. Concentrations ( $\mu\text{M}$ ) of THF. Spectrophotometric recordings of dopachrome accumulation in the action of 42 nM TYR on 0.5 mM L-DOPA in 30 mM sodium phosphate buffer (pH 7.0) at 25 °C. THF added at ( $\mu\text{M}$ ) (a) 0, (b) 10, (c) 20, (d) 40, and (e) 50. (Inset A) Action of THF and DHF on diphenolase activity of TYR. Spectrophotometric recording of dopachrome accumulated in the action of 42 nM TYR on 1 mM L-DOPA in 30 mM sodium phosphate buffer (pH 7.0) at 25 °C: (a) 1 mM L-DOPA, (b) 1 mM L-DOPA and 100  $\mu\text{M}$  THF, and (c) 1 mM L-DOPA and 100  $\mu\text{M}$  DHF. (Inset B) Action of THF on monophenolase activity of TYR. Spectrophotometric recordings of dopachrome accumulation in the action of 170 nM TYR on 0.25 mM L-tyrosine in 30 mM sodium phosphate buffer (pH 7.0) at 25 °C. THF added at ( $\mu\text{M}$ ) (a) 0, (b) 20, (c) 40, (d) 60, and (e) 80.

The experimental study was carried out in three steps following the methodology used to study the kinetics of suicide substrates.<sup>32</sup>

*Step 1: Preliminary Assays in Which the Stability of THF and DHF in the Experimental Conditions Used Was Investigated and Which Showed That They Were Stable in the Experimental Time (Results Not Shown).* Subsequently, the enzyme concentration was optimized, so that THF consumed and DHF formed fulfilled  $[\text{DHF}]_{\infty} \ll [\text{O}_2]_0$  and  $[\text{THF}]_0$  (results not shown).

*Step 2: Variation in Enzyme Concentration.* The concentrations of  $[\text{E}]_0$  were varied, while the substrate concentration was kept constant. The results are shown in Figure 1, while the inset of Figure 1 shows the dependence of  $\lambda_{\text{E}_{\text{ox}}^{\text{THF}}}$  and  $[\text{DHF}]_{\infty}$  with respect to the enzyme concentration. From the value of the slope of the relationship  $[\text{DHF}]_{\infty}$  versus  $[\text{E}]_0$ , the value of ( $r = 59.7 \pm 4.3$ ) is obtained, taking into account that, according to eq 2, the slope is  $2r$  (Table 1) [Note the low value of the parameter  $r$  (Table 1), which is one of the lowest described in the literature for this enzyme].<sup>22,23,30</sup> The values described for 7,8,4'-trihydroxyisoflavone and 5,7,8,4'-tetrahydroxyisoflavone are  $81.7 \pm 5.9$  and  $39.5 \pm 3.8$ , respectively,<sup>22</sup> and in the case of 8-hydroxyningenin, the value is  $283 \pm 21$ .<sup>23</sup>

*Step 3: Variation of the Concentration of THF.* With a fixed concentration of enzyme sufficient to give  $[\text{DHF}]_{\infty} \ll [\text{THF}]_0$  for the lowest substrate concentration being assayed, the concentration of THF was varied, while the concentration of  $\text{O}_2$  was kept constant at a saturating 0.26 mM (Figure 2). For the substrate studied, a hyperbolic dependence of the apparent

inactivation constant ( $\lambda_{\text{E}_{\text{ox}}^{\text{THF}}}$ ) was obtained with respect to the concentration of THF (inset of Figure 2).

Nonlinear regression analysis of  $\lambda_{\text{E}_{\text{ox}}^{\text{THF}}}$  versus  $[\text{THF}]_0$  according to eq 3 gave the values of  $\lambda_{\text{E}_{\text{ox}}^{\text{THF}}(\text{max})}$ , the apparent maximum inactivation constant, and  $K_{\text{m}}^{\text{THF}}$ , the Michaelis constant of TYR for THF (Table 1). From these values and taking into consideration eq 2, the catalytic constant,  $k_{\text{cat}}^{\text{THF}}$ , can be obtained (see Table 1). The value obtained for  $\lambda_{\text{E}_{\text{ox}}^{\text{THF}}(\text{max})}$ ,  $30 \pm 2 \times 10^{-3} \text{ s}^{-1}$ , is the highest described in the literature,<sup>21,22,30</sup> meaning that THF is a powerful suicide substrate for TYR, with a suicide potency,  $\lambda_{\text{max}}^{\text{THF}}/K_{\text{m}}^{\text{THF}}$ , of  $0.048 \pm 0.071 \text{ mM}^{-1} \text{ s}^{-1}$ .

The inactivation mechanism (Scheme 2) is consistent with the experimental observation that 50% of the copper is lost from the active site in the form of  $\text{Cu}^0$  during catechol inactivation<sup>33</sup> and also with the experiments carried out,<sup>34</sup> concerning the impossibility of reactivating the inactivated enzyme by adding  $\text{Cu}^{2+}$ , which, in turn, suggests the need for a "caddie" protein.<sup>35</sup> This could be a possible explication of the suicide inactivation of the enzyme.

**Inhibition of Browning through Reduction of *o*-Dopaquinone: Effect of THF on the Diphenolase and Monophenolase Activities of TYR.** The product of the action of TYR on L-tyrosine and L-DOPA (*o*-dopaquinone) acts as an oxidant of THF, because the redox potentials are *o*-dopaquinone/DOPA = 0.152 V and DHF/THF = -0.332 V at pH 7. At acid values (pH 4.5), both potentials shift approximately 0.18 V toward more positive values.<sup>29</sup> This was observed when both TYR activities (diphenolase and monophenolase) were studied in the presence of THF.

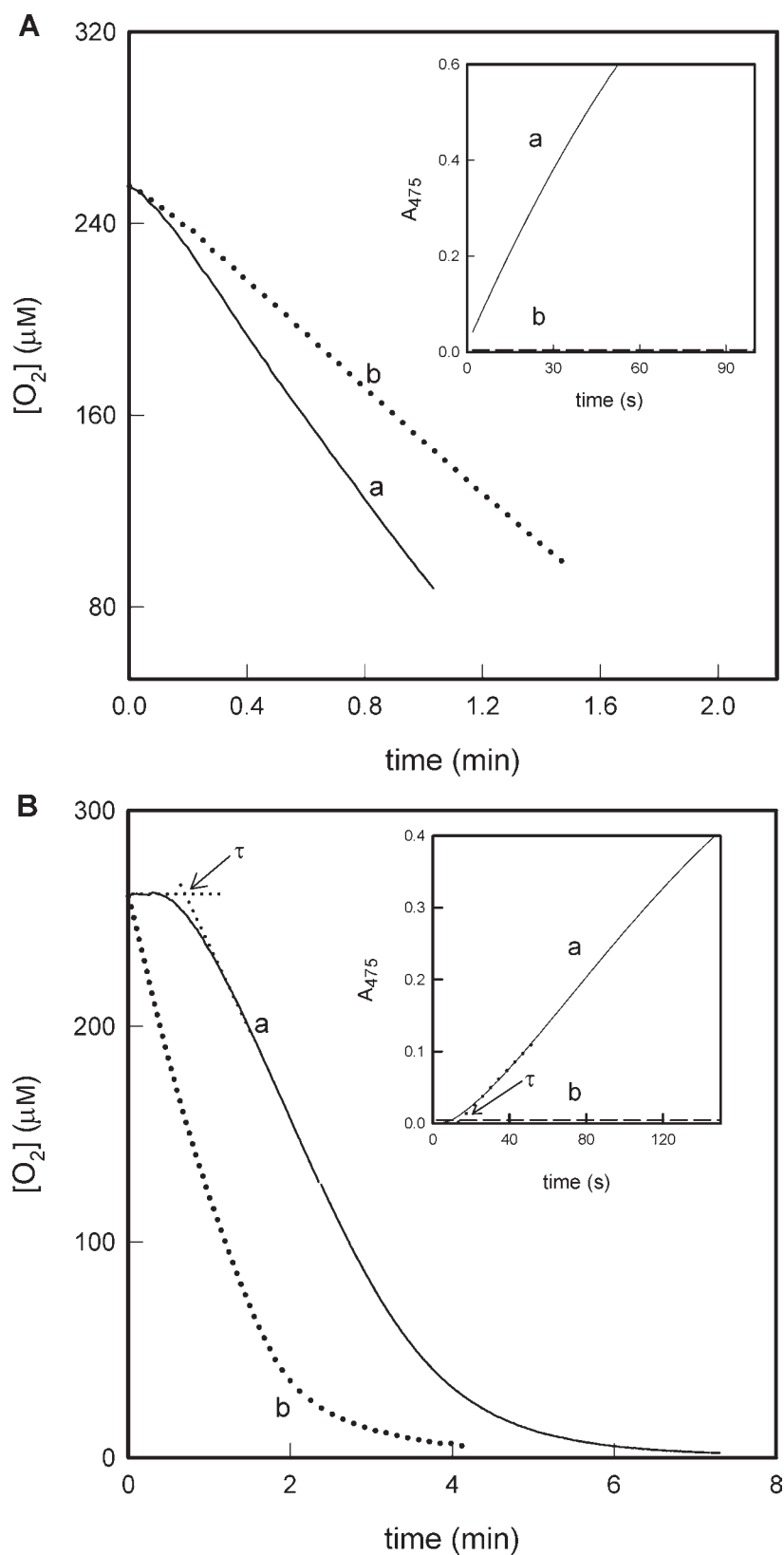


**Figure 4.** (A) Action of THF on diphenolase activity of TYR. Concentration (mM) of THF. Recordings of the oxygen consumption in the action of 42 nM TYR on 0.5 mM L-DOPA in 30 mM phosphate buffer (pH 7.0) at 25 °C. THF added at (mM) (a) 0 and (b) 0.6. (Inset A) Spectrophotometric recordings of dopachrome accumulation in the action of TYR on 0.5 mM L-DOPA in the same experimental conditions. THF added at (mM) (a) 0 and (b) 0.6. (B) Action of THF on monophenolase activity of TYR. Concentrations (mM) of THF. Recordings of oxygen consumption in the action of 170 nM TYR on 0.25 mM L-tyrosine in 30 mM sodium phosphate buffer (pH 7.0) at 25 °C. THF added at (mM) (a) 0 and (b) 0.75. (Inset B) Spectrophotometric recordings of dopachrome accumulation in the action of TYR on L-tyrosine in the same experimental conditions but with 250 nM TYR. THF added at (mM) (a) 0 and (b) 0.6.

The effect of THF, mediated by the reduction of *o*-dopaquinone, depends upon the concentration used. We shall therefore consider two cases.

**Low Concentrations of THF.** Figure 3 depicts the effect of THF at low ( $\mu\text{M}$ ) concentrations on the diphenolase activity, as seen by measuring dopachrome accumulation (Figure 3). The lag in dopachrome accumulation (recordings b–e in Figure 3) was due to the reduction of *o*-dopaquinone. Once THF has been consumed, dopachrome is accumulated at a rate ( $V_{0,D}^{\text{DC}}$ ) equal to the recording a obtained in the absence of THF. Note that *o*-dopaquinone does not oxidize DHF, as seen from inset A of Figure 3. This figure shows how *o*-dopaquinone oxidizes THF but not DHF. Recording a depicts the accumulation of dopachrome in the absence of THF or DHF. Recording b shows that the presence of THF leads to a lag, as described in recordings b–e of Figure 3. Recording c depicts the same experiment in the presence of DHF (no lag).

The effects of low concentrations of THF ( $\mu\text{M}$ ) on the action of the enzyme on L-tyrosine are depicted in inset B of Figure 3. For recording a of inset B of Figure 3, THF was not added. When dopachrome accumulation was measured (recordings a–e in inset B of Figure 3), the lag period diminished for lower concentrations of THF (recordings b and c in inset B of Figure 3), because *o*-diphenol accumulated in the medium more rapidly.<sup>16,17</sup> However, at higher concentrations, the lag was longer (recordings d and e in inset B of Figure 3), although the steady-state rates ( $V_{0,M}^{\text{DC}}$ ) were the same as in recording a.

**High Concentrations of THF.** In the case of TYR acting on *o*-diphenol, L-DOPA, when THF is in the order of millimolar concentrations, the oxygen consumption rate is inhibited [recordings in the (a) absence of THF and (b) presence of millimolar THF in Figure 4A]. The dopachrome accumulation rate is 0 (recording b in inset A of Figure 4), because *o*-quinone (Q) is reduced to *o*-diphenol (D) by THF. The reduced oxygen consumption rate (recording b in Figure 4A) may be explained by THF acting as a competitive inhibitor or as alternative substrate to L-DOPA.

When the monophenolase activity was measured following oxygen consumption at high concentrations of THF (mM) (Figure 4B), the lag disappeared, as can be seen in recording b. In recording a, there is no added THF. When dopachrome accumulation was measured (recording a in inset B of Figure 4), a zero rate was obtained (recording b) as a consequence of *o*-dopaquinone being reduced to L-DOPA by the addition of THF. On the basis of these experiments, especially that reflected in recording b of Figure 4B, it is deduced that THF reacts with the  $E_m$  form of the enzyme, thus eliminating the lag, and that the enzyme reaches a pseudo-steady state with a rate (recording b) similar that occurring in the absence of THF (recording a).

**Behavior of THF as the TYR Substrate: Enzymatic Catalysis.** THF may be oxidized (as a substrate) by TYR according to the kinetic mechanism proposed in Scheme 3, which depicts the enzymatic steps (Scheme 3a) and the reducing power of THF by non-enzymatic steps (Scheme 3b), (see Schemes 2 and 4). In this way, THF behaves as a competitive inhibitor of L-tyrosine and L-DOPA. This enzymatic activity can be measured by following the consumption of oxygen or the formation of DHF.

**Effect of pH.** With regard to the initial velocities, the THF oxidase activity of TYR increases with pH up to pH 3.2, above which it decreases, providing a broad peak at pH 3.2–4.0 (● in Figure 5). The pH dependence of this activity is contrary to that involved in the action of the enzyme on *o*-diphenols (■ in

**Scheme 3. Action of TYR on Monophenols and *o*-Diphenols in the Presence of THF**

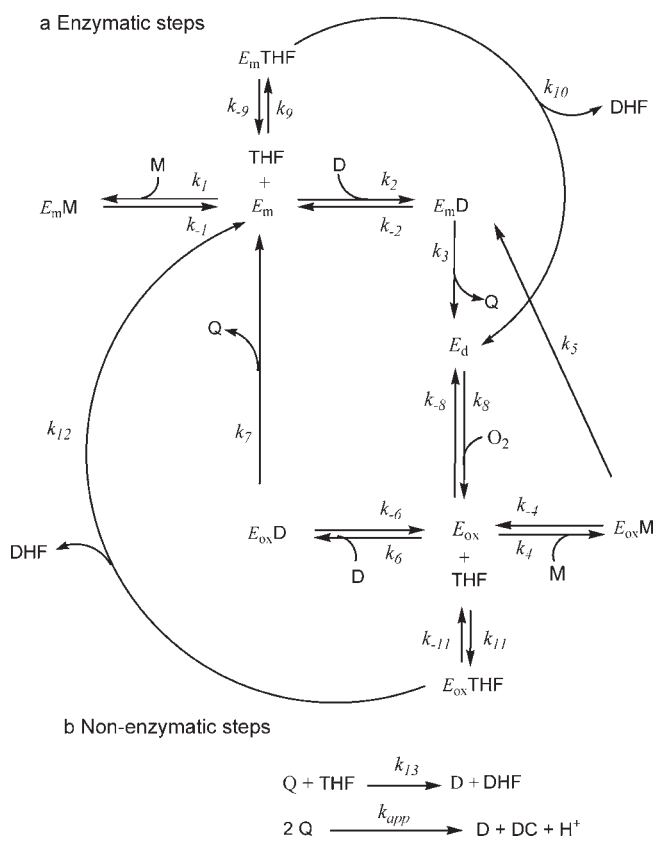


Figure 5). Furthermore, the shape of the curve reflects a  $pK_a$  close to that of diphenolase activity (■ in Figure 5), which suggests that the catalytic mechanism on *o*-diphenols and on this coenzyme is similar, only differing in the protonation–deprotonation of the substrate. From the kinetic analysis described in the Supporting Information, the DHF formation rate can be obtained as a function of  $[H^+]$ , as described in eq 5

$$V_{0,THF}^{\text{DHF}} = \frac{a[H^+]}{b + c[H^+] + [H^+]^2} \quad (5)$$

where  $V_{0,THF}^{\text{DHF}}$  is the initial formation rate of DHF from THF. Equation 5 shows the analytic expression of the variation in the enzyme reaction rate versus pH and agrees with the results shown in Figure 5. The expressions of  $a$ ,  $b$ , and  $c$  are indicated in eqs 3SM–5SM of the Supporting Information.

**Proposed Structural Mechanism To Explain the Catalysis and Suicide Inactivation of TYR in Its Action on THF.** The proposed structural mechanism to explain the catalysis and suicide inactivation of TYR in its action on THF is depicted in Scheme 4.

From studies of the effect of pH on the enzyme activity measured at short times (Figure 5 and the Supporting Information), it can be deduced that the substrate must become protonated for it to bind to the enzyme. In step 1, the enzyme in the  $E_m$  form binds to the substrate, possibly establishing a hydrogen bridge between the base B and the hydrogen bound to the nitrogen of



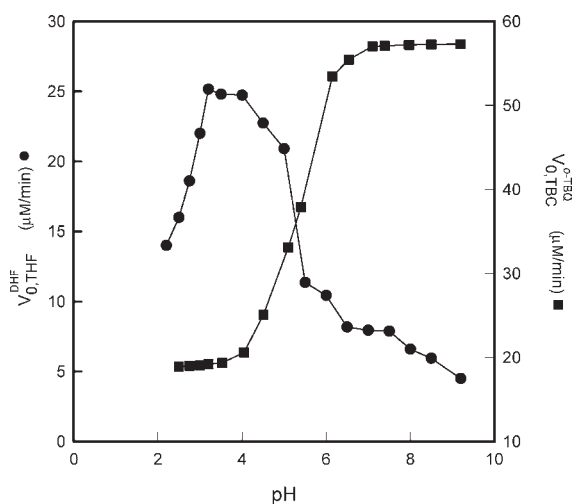


**Figure 5.** Effect of pH on the oxidation rate of THF by TYR. (●) Representation of  $V_{0,THF}^{DHF}$  versus pH. The experimental conditions were 30 mM sodium acetate buffer at pH 2.2, 2.5, 2.75, 3.0, 3.2, 3.5, 4.0, 4.5, and 5.0 and 30 mM sodium phosphate buffer at pH 5.5, 6.0, 6.5, 7.0, 7.5, 8.0, 8.5, and 9.2, 62.5  $\mu\text{M}$  THF, 0.26 mM  $\text{O}_2$ , and 400 nM TYR. (■) Effect of pH on the oxidation of TBC by TYR. Representation of  $V_{0,TBC}^{o-TBC}$  versus pH with 2 mM TBC and 2.5 nM TYR. The buffers used were the same as for tetrahydrofolate oxidase activity.

the pteridin ring. In step 2, the nitrogen of the ring, which is a powerful nucleophile because  $\text{C}_{4a}$  has a low value of  $\delta_{4a}$  (Table 1) and, therefore, a high electron density, can carry out a nucleophilic attack on the copper of the active site, binding axially, while the hydrogen, which is bound to the nitrogen, is withdrawn by base B. In step 3, OH of the substrate transfers a proton to histidine, binding biaxially, before oxidation/reduction processes governed by step 4 originate the form  $\text{E}_d$ . Because of the low  $K_m^2$  and the high oxygen concentration in the medium,  $\text{E}_d$  becomes  $\text{E}_{ox}$  (step 5), with  $\text{Cu}^{2+}\text{Cu}^{2+}$  and a peroxide group co-planar with both copper atoms. Subsequently, the form  $\text{E}_{ox}$  binds to another molecule of protonated substrate (step 6), which, through the nitrogen atom, carries out a nucleophilic attack on the copper atom. In step 7, the proton of the hydroxyl group is transferred from the substrate to the peroxide and hydrogen bound to the nitrogen is transferred to the oxygen of the hydroxyl, while the intermediate formed may transfer hydrogen in two ways (steps 8 and 10). In step 8, the most rapid, hydrogen is transferred to nitrogen of the histidine, with the subsequent nucleophilic attack of oxygen on the copper atom, giving rise to the intermediate  $(\text{E}_{ox}-\text{THF})_2$ . In step 10, the hydrogen atom is transferred to the peroxide, giving rise to the complex  $(\text{E}_{ox}-\text{THF})_3$ . This last step is slower than step 8 because the oxygen atom of the peroxide, as a result of the binding of the first hydrogen atom in step 7, has a certain positive charge density. The following reactions arise from these complexes: an oxidation/reduction step through step 9 in the case of complex  $(\text{E}_{ox}-\text{THF})_2$ , releasing the form  $\text{E}_m$  and the product DHF, and, through step 11, the reduction of a  $\text{Cu}^{2+}$  atom to  $\text{Cu}^0$  by means of the electron transport described in  $(\text{E}_{ox}-\text{THF})_3$ , releasing the inactive form of the enzyme  $\text{E}_i$  and the product DHF.

**Inhibition of Browning in the Presence of THF.** Browning and pigmentation may diminish in the presence of THF. Browning may be inhibited in three ways: first, by irreversibly inhibiting the enzyme TYR by acting as a suicide substrate, second, by acting as a competitive substrate of monophenols and *o*-diphenols

for the enzyme, and last, by acting as a reductant of *o*-quinone. In the short term, the most effective mechanism for inhibiting browning could be the reduction of *o*-quinones by THF, although the most long-lasting process would be the suicide inactivation of the enzyme.

## ASSOCIATED CONTENT

**S Supporting Information.** Kinetic analysis of the pH effect on the enzymatic activity. This material is available free of charge via the Internet at <http://pubs.acs.org>.

## AUTHOR INFORMATION

### Corresponding Author

\*Fax: +34-868883963. E-mail: [canovasf@um.es](mailto:canovasf@um.es).

### Funding Sources

This paper was partially supported by grants from the Ministerio de Educación y Ciencia (Madrid, Spain) Projects BIO2009-12956, CTQ2009-13023, and SAF2009-12043-C02-01 and the Fundación Séneca (CARM, Murcia, Spain) Projects 08856/PI/08, 08813/PI/08, and 08595/PI/08. Jose Luis Muñoz-Muñoz and Francisco García-Molina hold two fellowships from the Fundación Caja Murcia (Murcia, Spain).

## REFERENCES

- (1) Prota, G.; Ischia, M.; Napolitano, A. In *The Chemistry of Melanins and Related Metabolites*; Nordlund, J. J., Boissy, R. E., Hearing, V. J., King, R. A., Ortonne, J. P., Eds.; Oxford University Press: New York, 1988.
- (2) Solomon, E. I.; Sundaram, U. M.; Machonkin, T. E. Multicopper oxidases and oxygenases. *Chem. Rev.* **1996**, *96*, 2563–2606.
- (3) Whitaker, J. R.; Lee, C. Y. In *Recent Advances in Chemistry of Enzymatic Browning: An Overview*; Lee, C. Y., Whitaker, J. R., Eds.; American Chemical Society (ACS): Washington, D.C., 1995; ACS Symposium Series, Vol. 600, Chapter 1, pp 2–7.
- (4) Van Gelder, C. W.; Flurkey, W. H.; Wichers, H. J. Sequence and structural features of plant and fungal tyrosinases. *Phytochemistry* **1997**, *45*, 1309–1323.
- (5) Bubacco, L.; Salgado, J.; Tepper, A. W.; Vijgenboom, E.; Canters, G. W.  $^1\text{H}$  NMR spectroscopy of the binuclear Cu(II) active site of *Streptomyces antibioticus* tyrosinase. *FEBS Lett.* **1999**, *442*, 215–220.
- (6) Ohguchi, K.; Tanaka, T.; Iliya, I.; Ito, T.; Linuma, M.; Matsumoto, K.; Akao, Y.; Nozawa, Y. Gnetol as a potent tyrosinase inhibitor from genus *Gnetum*. *Biosci., Biotechnol., Biochem.* **2003**, *67*, 663–665.
- (7) Briganti, S.; Camera, E.; Picardo, M. Chemical and instrumental approaches to treat hyperpigmentation. *Pigm. Cell Res.* **2003**, *16*, 101–110.
- (8) Solano, F.; Briganti, S.; Picardo, M.; Ghanem, G. Hypopigmenting agents: An updated review on biological, chemical and clinical aspects. *Pigm. Cell Res.* **2006**, *19*, 550–571.
- (9) Rezk, B. M.; Haenen, G. M.; van der Vijgh, W. J.; Bast, A. Tetrahydrofolate and 5-methyltetrahydrofolate are folates with high antioxidant activity. Identification of the antioxidant pharmacophore. *FEBS Lett.* **2003**, *555*, 601–605.
- (10) Gliszczynska-Swiglo, A.; Muzolf, M. pH-Dependent radical scavenging activity of folates. *J. Agric. Food Chem.* **2007**, *55*, 8237–8242.
- (11) Hanson, A. D.; Roje, S. One-carbon metabolism in higher plants. *Annu. Rev. Plant Physiol. Plant Mol. Biol.* **2001**, *52*, 119–137.
- (12) Sahr, T.; Ravel, S.; Rébeillé, F. Tetrahydrofolate biosynthesis and distribution in higher plants. *Biochem. Soc. Trans.* **2005**, *33*, 758–762.
- (13) Bailey, L. B.; Gregory, J. F., III. Folate metabolism and requirements. *J. Nutr.* **1999**, *129*, 779–782.
- (14) Scott, J.; Rébeillé, F.; Fletcher, J. Folic acid and folates: The feasibility for nutritional enhancement in plant foods. *J. Sci. Food Agric.* **2000**, *80*, 795–824.



- (15) Florez, J. In *Farmacologia Humana*; Florez, J., Armijo, J. A., Mediavilla, A., Eds.; Masson: Barcelona, Spain, 1997; p 102S.
- (16) Vaughan, P. F.; Butt, V. S. The hydroxylation of *p*-coumaric acid by an enzyme from leaves of spinach beet (*Beta vulgaris* L.). *Biochem. J.* **1969**, *113*, 109–115.
- (17) García-Molina, F.; Muñoz-Muñoz, J. L.; García-Molina, M.; García-Ruiz, P. A.; Tudela, J.; García-Canovas, F.; Rodríguez-Lopez, J. N. Melanogenesis inhibition due to NADH. *Biosci., Biotechnol., Biochem.* **2010**, *74*, 1777–1787.
- (18) García-Molina, F.; Muñoz-Muñoz, J. L.; Acosta, J. R.; García-Ruiz, P. A.; Tudela, J.; García-Canovas, F.; Rodríguez-Lopez, J. N. Melanogenesis inhibition by tetrahydropterines. *Biochim. Biophys. Acta* **2009**, *1794*, 1766–1774.
- (19) Reish, O.; Townsend, D.; Berry, S. A.; Tsai, M. Y.; King, R. A. Tyrosinase inhibition due to interaction of homocyst(e)ine with copper: The mechanism for reversible hypopigmentation in homocystinuria due to cystathionine  $\beta$ -synthase deficiency. *Am. J. Hum. Genet.* **1995**, *57*, 127–132.
- (20) Shaker, O. G.; El-Tahlawi, S. M. R. Is there a relationship between homocysteine and vitiligo? A pilot study. *Br. J. Dermatol.* **2008**, *159*, 720–724.
- (21) Jimbow, K.; Chen, H.; Park, J. S.; Thomas, P. D. Increased sensitivity of melanocytes to oxidative stress and abnormal expression of tyrosinase-related protein in vitiligo. *Br. J. Dermatol.* **2001**, *144*, 55–65.
- (22) Chang, T. S. Two potent suicide substrates of mushroom tyrosinase: 7,8,4'-Trihydroxyisoflavone and 5,7,8,4'-tetrahydroxyisoflavone. *J. Agric. Food Chem.* **2007**, *55*, 2010–2015.
- (23) Chang, T. S.; Lin, M. Y.; Lin, H. J. Identifying 8-hydroxynaringenin as a suicide substrate of mushroom tyrosinase. *J. Cosmet. Sci.* **2010**, *61*, 205–210.
- (24) Rodríguez-López, J. N.; Fenoll, L. G.; García-Ruiz, P. A.; Varón, R.; Tudela, J.; Thorneley, R. N.; García-Cánovas, F. Stopped-flow and steady-state study of the diphenolase activity of mushroom tyrosinase. *Biochemistry* **2000**, *39*, 10497–10506.
- (25) Bradford, M. M. A rapid and sensitive method for the quantitation of microgram quantities of protein utilizing the principle of protein–dye binding. *Anal. Biochem.* **1976**, *72*, 248–254.
- (26) García-Molina, F.; Muñoz-Muñoz, J. L.; Varon, R.; Rodríguez-Lopez, J. N.; García-Cánovas, F.; Tudela, J. A review on spectrophotometric methods for measuring the monophenolase and diphenolase activities of tyrosinase. *J. Agric. Food Chem.* **2007**, *55*, 9739–9749.
- (27) Rodríguez-López, J. N.; Ros-Martínez, J. R.; Varón, R.; García-Cánovas, F. Calibration of a Clark-type oxygen electrode by tyrosinase-catalyzed oxidation of 4-*tert*-butylcatechol. *Anal. Biochem.* **1992**, *202*, 356–360.
- (28) Jandel Scientific. *Sigma Plot 9.0 for Windows*; Jandel Scientific: Core Madera, CA, 2007.
- (29) Mirčeski, V.; Komorsky-Lovrić, S.; Lovrić, M. *Square Wave Voltammetry. Theory and Application*; Springer: New York, 2008.
- (30) Muñoz-Muñoz, J. L.; García-Molina, F.; García-Ruiz, P. A.; Molina-Alarcon, M.; Tudela, J.; García-Canovas, F.; Rodríguez-Lopez, J. N. Phenolic substrates and suicide inactivation of tyrosinase: Kinetics and mechanism. *Biochem. J.* **2008**, *416*, 431–440.
- (31) Fenoll, L. G.; Rodríguez-López, J. N.; García-Molina, F.; García-Cánovas, F.; Tudela, J. Michaelis constants of mushroom tyrosinase with respect to oxygen in the presence of monophenols and diphenols. *Int. J. Biochem. Cell Biol.* **2002**, *34*, 332–336.
- (32) Tudela, J.; García-Canovas, F.; Varon, R.; Jiménez, M.; García-Carmona, F. Kinetic characterization of dopamine as a suicide substrate of tyrosinase. *J. Enzyme Inhib.* **1987**, *2*, 47–56.
- (33) Dietler, C.; Lerch, K. In *Oxidases and Related Redox Systems*; King, T. E., Mason, H. S., Morrison, M., Eds.; Pergamon Press: New York, 1982; pp 305–317.
- (34) Land, E. J.; Ramsden, C. A.; Riley, P. A. The mechanism of suicide-inactivation of tyrosinase: A substrate structure investigation. *Tohoku J. Exp. Med.* **2007**, *212*, 341–348.
- (35) Matoba, Y.; Kumagai, T.; Yamamoto, A.; Yoshitsu, H.; Sugiyama, M. Crystallographic evidence that the dinuclear copper center of tyrosinase is flexible during catalysis. *J. Biol. Chem.* **2006**, *281*, 8981–8990.